

Magnetization reversal assisted by the inverse piezoelectric effect in Co-Fe-B/ferroelectric multilayers

Na Lei,^{*} Sanghwan Park, Philippe Lecoeur, Dafiné Ravelosona,[†] and Claude Chappert
Institut d'Electronique Fondamentale, UMR CNRS, and Université Paris–Sud, F-91405 Orsay, France

Olha Stelmakhovych and Vaclav Holý

Department of Condensed Matter Physics, Faculty of Mathematics and Physics, Charles University, Ke Karlovu 5, 121 16 Prague 2, Czech Republic

(Received 21 December 2010; revised manuscript received 24 March 2011; published 11 July 2011)

We investigate magnetization reversal assisted by electric fields in a $\text{Co}_{40}\text{Fe}_{40}\text{B}_{20}/\text{Co}/\text{Pd}$ multilayer with soft perpendicular anisotropy deposited onto an epitaxial piezoelectric layer. Both the nucleation and depinning magnetic fields show a strong reduction of up to 30% under the application of an electric field. These results show good prospects for assisting the switching processes in ultra-low-power spintronic devices.

DOI: [10.1103/PhysRevB.84.012404](https://doi.org/10.1103/PhysRevB.84.012404)

PACS number(s): 75.60.Jk, 75.30.Gw, 75.70.Kw, 77.55.fp

In recent years, spintronics has become increasingly important because of its potential applications for magnetic random access memory (MRAM), logic devices, and magnetoelectric sensors.^{1–4} In particular, the use of spin-transfer torque in devices with perpendicular anisotropy is attracting considerable interest because of their ability to reach ultrahigh density.⁵ This holds for current-driven domain-wall motion in magnetic tracks that promises record density and high speed.⁶ However, the critical current density to move domain walls is still too high for practical applications. Further reduction in the power consumption in these devices, while maintaining high thermal stability, remains a challenging problem.

One promising route to reduce power consumption is through the use of an electric field.⁴ Among different approaches to develop voltage-driven devices, the voltage control of magnetic anisotropy as a means to reduce the energy barrier for magnetization switching has attracted particular attention. That approach includes electrical field control of carrier density in semiconductor systems,^{7,8} high k electrolyte and insulator to change interfacial electronic states,^{9–11} and the magnetoelectric effect.^{12–14} For magnetoelectric coupling systems, ferroelectric materials are used to generate strain that is transferred to the magnetic layer.^{12,14} While most studies have focused on bulk actuators to manipulate the anisotropy, the use of piezoelectric film is a promising alternative as it can be integrated into hybrid magnetic-ferroelectric spintronic devices. This concept has been demonstrated in $\text{Pb}(\text{Zr}_x\text{Ti}_{1-x})\text{O}_3/\text{CoPd}$ systems where the perpendicular magnetic anisotropy can be manipulated using electric field.¹⁵

Here, we show that the inverse piezoelectric effect can be used to assist the nucleation and depinning process of magnetic domain walls in high-quality $\text{CoFeB}/\text{Co}/\text{Pd}$ films with perpendicular anisotropy. These results were made possible using an epitaxial $0.7(\text{PbMg}_{1/3}\text{Nb}_{2/3}\text{O}_3)-0.3(\text{PbTiO}_3)$ (PMN-PT) layer as the piezoelectric layer, due to its giant piezoelectric response.

PMN-PT (120 and 300 nm) films were epitaxially grown at 600 °C on $\text{La}_{0.67}\text{Sr}_{0.33}\text{MnO}_3$ (LSMO) (25 nm)/STO/Si(001) (Ref. 16) substrate by pulsed laser deposition (PLD). A KrF excimer laser of 248 nm wavelength was used with 2 Hz

repetition and about 2.2 mJ/cm² energy density in an O₂ ambient of 120 mTorr for LSMO deposition and in a N₂O ambient of 260 mTorr for PMN-PT deposition, followed by a cooling-down procedure under 300 Torr of pure oxygen atmosphere. Here a 25-nm-thick LSMO layer was used as a high-quality bottom electrode, which can be epitaxially grown on STO/Si(001) substrate.¹⁷ We have focused our study on soft CoFeB films exchange coupled to strong Co/Pd multilayers for the magnetic system. The main advantages of such hard and soft magnetic systems are that domain-wall (DW) motion occurs at very low propagation fields due to the amorphous character of CoFeB,¹⁸ and that this material is compatible with MgO-based tunnel junctions for further integration into spintronic devices.⁵ Finally, the magnetic multilayers, 3 (nm) Pd/0.2 Co/0.6 Pd/0.2 Co/1.7 Pd/0.54 CoFeB/3 Pd,¹⁹ were grown on top of the PMN-PT layer by magnetron sputtering with low Ar ambient of 5.8×10^{-4} mbar at room temperature. In these structures, Kerr microscopy measurements indicate that magnetization reversal is dominated by a high density of nucleation sites at H_N followed by DW propagation at $H_P > H_N$.²⁰ This makes these films a model system to study the influence of piezoelectric response on the mechanism of magnetization reversal. All the measurements described in the following were carried out at room temperature.

A typical θ - 2θ spectrum of a 120-nm-thick PMN-PT grown on LSMO/STO/Si(001) is shown in Fig. 1(a), indicating a purely (001) orientated perovskite structure. The morphology of the PMN-PT films was characterized by atomic force microscopy (AFM) measurements as shown in Fig. 1(b). The root-mean-square roughness is less than 2 nm, which promotes a sufficiently flat surface for the subsequent growth of the magnetic films. To characterize the ferroelectric properties of PMN-PT films, we have performed C - V measurements, for which a 25 nm LSMO and a 200-nm-thick Pt layer were used as the bottom and top electrodes, respectively. As shown in Fig. 1(c), the typical butterfly shape can be clearly seen with a very small coercivity. Note that the presence of a slight asymmetry may arise from the use of asymmetric electrodes. Figure 1(d) shows a measurement of the leakage current that is as low as 10^{-4} A/cm² at 0.1 kV/mm, indicating a high structural quality of the ferroelectric layer.

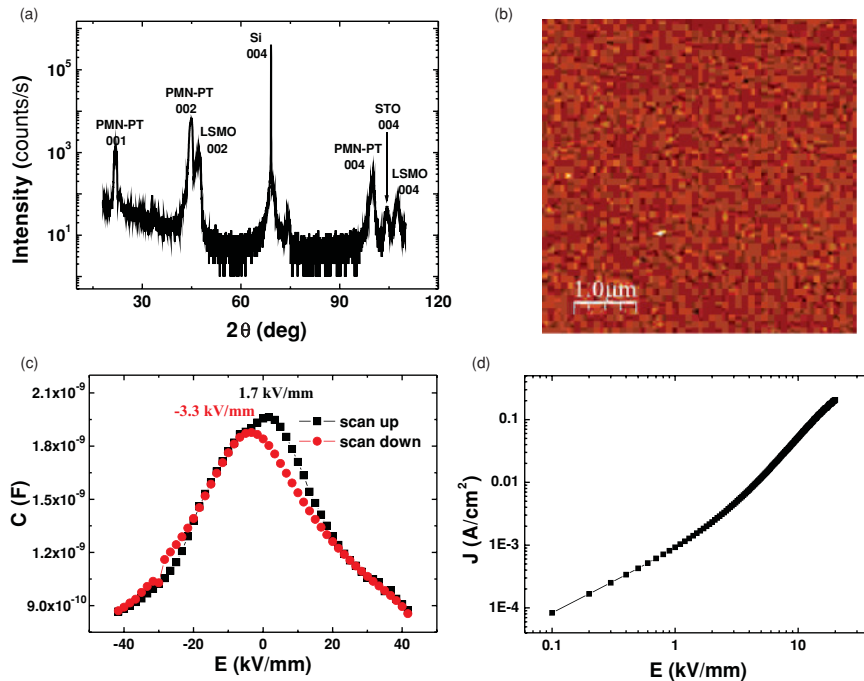


FIG. 1. (Color online) (a) θ - 2θ scan of 120 nm PMN-PT on LSMO/STO/Si(001) substrate. (b) AFM image with $5 \times 5 \mu\text{m}^2$ shows 2 nm root-mean-square roughness.²¹ (c) C - V measurement at 0.1 MHz: scanning up (from -5 to 5 V) is shown by squares, and scanning down is shown by circle dots. (d) I - V measurement shows leakage current density vs electric field.

The surface morphology after the magnetic layer growth on top of a PMN-PT (300 nm)/LSMO (25 nm)/STO (20 nm)/Si(001) structure is found to be highly improved. This feature is attributed to the smoothing of the surface when a 3-nm-thick Pd layer is deposited onto the piezoelectric layer. As a result, the hysteresis loop at zero applied voltage seen in Fig. 2(a) indicates the presence of perpendicular anisotropy with a typical low coercivity field of 32 Oe. All the MOKE measurements were performed at the same sweeping rate dH/dt . Based on a Kerr microscopy study,¹⁸ the magnetization reversal in these films is found to be dominated by a high density of nucleation sites at $H_N = 15$ Oe followed by a distribution of propagation fields $\Delta H_P = H_N - H_S$, where H_S is the saturation field. The coercivity field here corresponds then to the mean propagation field.

In the following, we describe the effect of an electric field applied onto the piezoelectric layer. Voltages up to 17 V were applied with the magnetic layer and LSMO layer serving as the top and bottom electrodes, respectively. Positive (negative) voltage is defined such that the electric field is pointing from bottom (top) to top (bottom) electrodes. Polar Kerr hysteresis loops measured as a function of the applied voltages are shown in Fig. 2(a). It is clear that the coercivity field H_C decreases with increasing the amplitude of the applied voltage, regardless of whether it is positive (solid dots) or negative (open dots). At an applied voltage of 17 V, the magnetization reversal process is much less abrupt, which indicates that the perpendicular anisotropy has been reduced. Figures 2(b), 2(c), and 2(d) show the variation of the nucleation field H_N , the mean propagation field H_P , and the distribution ΔH_P as a function of the applied voltage. The large reduction in H_P and H_N under the applied voltage is compatible with a reduction of the perpendicular anisotropy.²⁰ The abrupt variation of ΔH_P at $U > 10$ V corresponds to the onset of the transition from out-of-plane to in-plane magnetization as consistent with a recent study on irradiation-induced modification of perpendicular anisotropy

in similar films.²² At this transition, the magnetic films are highly inhomogeneous with a large distribution of in-plane and out-of-plane anisotropy, consistent with an increase of ΔH_P .

In the following, we discuss the origin of the modification of the magnetization reversal mechanism seen in Fig. 2. First, thermal effects may play an important role at high applied voltages. However, the value of the Kerr rotation at saturation is not modified under voltage, indicating that M_S remains constant. Furthermore, the magnitude of the current flowing into the structure under electric field was also verified to ascertain contribution of the Joule effect. Since the Schottky barrier between magnetic layer and PMN-PT induces a diode behavior, the current is expected to be much higher for negative voltage than positive voltage. As shown in Fig. 2(a), there is almost no difference in coercivity fields between $+4.7$ V (red solid diamonds) and -4.7 V (blue open circles) applied voltage, even though the current is three times larger for the latter case ($+4$ mA and -12.2 mA, respectively). However, the difference in coercivity field can be clearly seen between -4.7 V (blue open circles) and $+13$ V (pink solid diamonds) in applied voltage, although the amplitude of current is the same. This clearly shows that the coercivity change depends mainly on the amplitude of the electric field rather than the applied current.

Finally, electric-field-induced charge transfer¹¹ can also be excluded since a 3-nm-thick Pd layer is used at the interface between the magnetic layer and the PMN-PT layer. We therefore believe that our results are consistent with the inverse piezoelectric effect that generates strain into the magnetic layer. The large density of nucleation sites in our films is consistent with the presence of intrinsic defects where the value of the perpendicular magnetic anisotropy K_U is reduced. The nucleation field H_N that corresponds to the reversal of small magnetic volumes can be written as $H_N = K_{um}/2M_S$, where K_{um} corresponds to the minimum values of perpendicular anisotropy in the films.²³ Results of Fig. 2(b) indicate that K_{um} is reduced by about 30% under voltage of 10 V. From

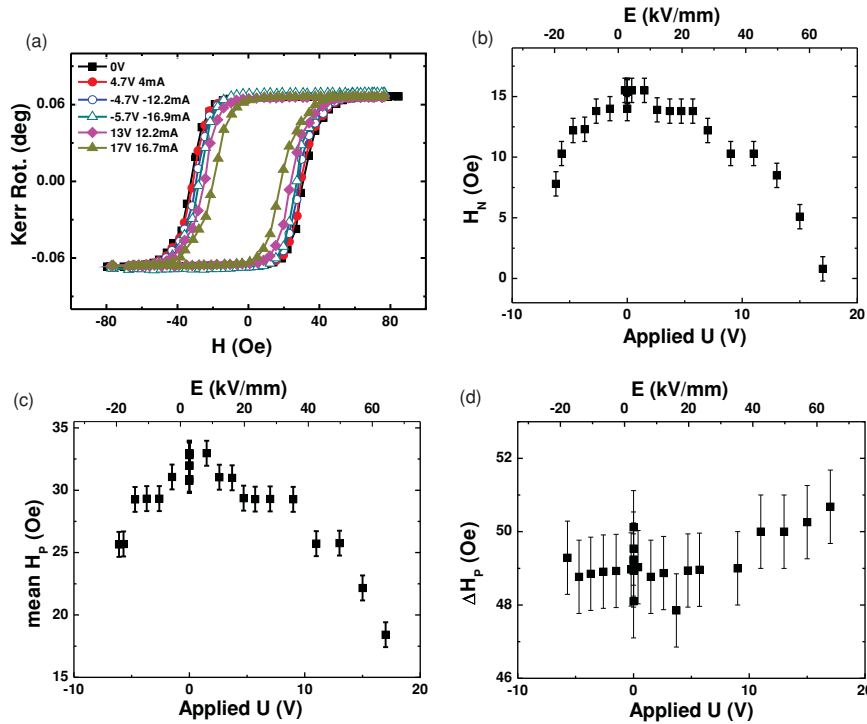


FIG. 2. (Color online) (a) Hysteresis loops with different applied voltages. (b) Nucleation fields with different applied voltages. (c) Mean propagation fields (coercivity fields) with different applied voltages. (d) Distribution of propagation fields with different applied voltages.

10 to 17 V it is not relevant to evaluate the variation of K_{um} through H_N since strong magnetic fluctuations are involved in the magnetization reversal process.

To go further in our analysis, the magnetic anisotropy field under electric field was measured using angle-dependent polar MOKE measurements.²⁴ An angle of 15° between magnetic field and sample surface was chosen and the corresponding hysteresis loops are shown in the inset of Fig. 3(a) for 0 and 17 V applied voltages, respectively. A slight reduction in the saturation field at an applied voltage of 17 V can be observed in Fig. 3(a). To extract the anisotropy field, we used a fitting procedure based on an anisotropy energy density model: $E = -2\pi M_S^2 \cos^2 \theta + K_1 \cos^2 \theta + K_2 \cos^4 \theta - H \cdot M_S \cos(\theta - \phi)$, where θ is the angle between M and the surface plane and ϕ is the angle between H and the surface plane. By energy minimization, $dE/d\theta = 0$, the field dependence can be deduced as $H = (H_a \sin \theta \cos \phi + H_b \sin^3 \theta \cos \phi) / \sin(\theta - \phi)$, in which $H_a = 2(K_1 - 2\pi M_S^2 + 2K_2) / M_S$ and $H_b = -4K_2 / M_S$. The fitting results are shown by the solid curves, which give $H_a = 3450$ Oe and $H_b = -1500$ Oe at zero applied voltage. Since the strain effect is expected to mainly change the

uniaxial term, we have kept the high-order coefficient H_b as constant for the fitting procedure at 17 V. As a result, we obtained $H_a = 3100$ Oe at 17 V. Compared with zero applied voltage, the anisotropy field is found to decrease by about 10%.

Here, such a MOKE measurement gives the anisotropy change of the full film at saturation, which corresponds to the highest value of the anisotropy in the films. On the contrary, as seen above, the anisotropy deduced from the nucleation fields is related to the lowest values of the anisotropy distribution. This could explain the difference in the reduction of anisotropy obtained from the two methods (30% versus 10%).

Finally, to characterize the strain amplitude, XRD measurements were performed with 0 and 17 V applied voltages, respectively. For PMN-PT, the strain along the c axis is expected to be positive when the applied electrical field is higher than the electric switching field. This explains why the electric-field-induced anisotropy change is symmetric: either the voltage is positive or negative. Based on the shift of the PMN-PT (002) peak seen in Fig. 3(b), a strain of 0.025% can be extracted at 17 V, which is a reasonable value for thin films compared with the strain measurement in PMN-PT single-crystal substrate.²⁵ It is worth noting that

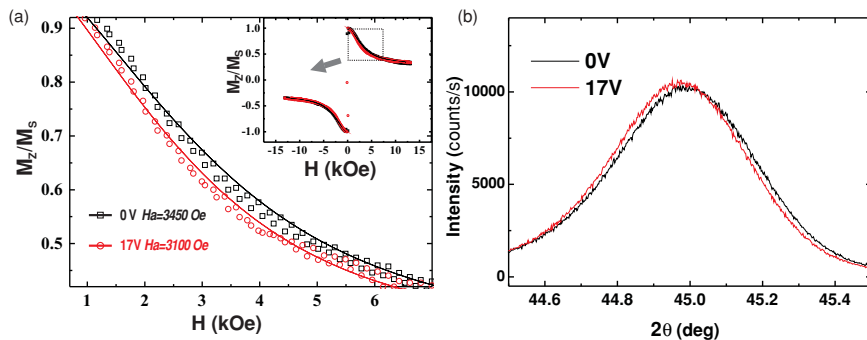


FIG. 3. (Color online) (a) Zoom of the square area of the inset figure. Inset: Normalized out-of-plane magnetization vs magnetic field at 0 V (open square), +17 V (open circle) applied, and fitting results (solid curves). (b) XRD spectra of PMN-PT 002 peak at 0 V (black) and 17 V (red), respectively.

the XRD measurement gives an average strain within the whole film, whereas the real strain transferred to the magnetic layer depends on the top part of the PMN-PT layer, which is presumably larger than 0.025% due to the strain relaxation in the piezoelectric films. Our results are consistent with a negative magnetostriction coefficient of the magnetic layer, i.e., the perpendicular anisotropy decreases when a positive strain is applied along the c axis.

In the following, we made the simple hypothesis that the strain induced in the PMN-PT layer generates a homogeneous strain in the whole Pd/(Co/Pd)/CoFeB/Pd stack. In addition, we have considered independently the magnetostriction of the Co/Pd multilayer and that of the single CoFeB layer to calculate the average change in magnetic anisotropy. The strain-induced anisotropy can be written as $K_e = -\frac{3}{2}\lambda\sigma$, $\sigma = \varepsilon E_f / (1 - \nu^2)$, where λ is the magnetostriction coefficient, ε is the strain, E_f is Young's modulus, and ν is the Poisson ratio. Based on previous study of the Co/Pd multilayer,²⁶ we took $\lambda = -1.5 \times 10^{-4}$ and $E_f = 1.5 \times 10^{12}$ dyn/cm². For CoFeB, we considered $\lambda = 2 \times 10^{-5}$,²⁷ $E_f = 1.6 \times 10^{12}$ dyn/cm²,²⁸ and the typical value of ν for metals is around 0.3. The strain generated by the PMN-PT corresponds to in-plane compression²⁹ and it is transferred to the magnetic layer as $\varepsilon_{\perp} = -2\nu\varepsilon_{\parallel} / (1 - \nu)$, where $\nu = 0.5$ for PMN-PT.³⁰ We found $\varepsilon_{\parallel} = -0.0125\%$ based on XRD measurements. Finally, the strain-induced anisotropy changes

in Co/Pd and CFB are $K_e^{\text{CoPd}} = -4.6 \times 10^4$ erg/cm³ and $K_e^{\text{CFB}} = 0.66 \times 10^4$ erg/cm³, respectively. Taking into account the relative thicknesses of the CoPd multilayer and of CFB, we found a strain-induced anisotropy change of $K_e = -3.72 \times 10^4$ erg/cm³. Taking the measured value of $K = 8 \times 10^5$ erg/cm³ for CoFeB/Co/Pd,¹⁸ the change of anisotropy is found to be about 5%. This estimated value is consistent with the 10% variation given by the MOKE measurement, taking into account that the measured value $\varepsilon_{\perp} = 0.025\%$ underestimates the strain transferred to the magnetic layer and the simplicity of the model used.

In summary, high-quality ferroelectric PMN-PT films have been used to tune magnetic perpendicular magnetic anisotropy using an electrical field. A substantial reduction in the propagation and nucleation fields for domain walls has been found under applied voltages of Co-Fe-B/PMN-PT multilayers. These results are promising for a magnetic switching assisted with an electric field in low-power nanodevices.

We thank Dr. B. Vilquin (INL/UMR5270, Ecole Centrale de Lyon) for supplying the STO/Si(001) substrates and Dr. Mai Pham Thi (Thales TRT) for the PMN-PT target fabrication. This work is supported by the EC program NMP under STREP Contract No. 214499 NAMASTE. N.L. acknowledges financial support from the regional government of Ile-de-France through C'Nano IdF grant.

*na.lei@u-psud.fr

†dafine.ravelosona@u-psud.fr

¹I. Žutić, J. Fabian, and S. Das Sarma, *Rev. Mod. Phys.* **76**, 323 (2004).

²S. A. Wolf *et al.*, *Science* **294**, 1488 (2001).

³S. Priya *et al.*, *Sensors* **9**, 6362 (2009).

⁴C. Chappert, A. Fert, and F. Nguyen Van Dau, *Nat. Mater.* **6**, 813 (2007).

⁵S. Ikeda *et al.*, *Nat. Mater.* **9**, 721 (2010).

⁶C. Burrowes *et al.*, *Nat. Phys.* **6**, 17 (2010).

⁷D. Chiba *et al.*, *Nature (London)* **455**, 515 (2008).

⁸I. Stolicnov *et al.*, *Nat. Mater.* **7**, 464 (2008).

⁹M. Weisheit *et al.*, *Science* **315**, 349 (2007).

¹⁰T. Maruyama *et al.*, *Nature Nanotech.* **4**, 158 (2009).

¹¹M. Endo *et al.*, *Appl. Phys. Lett.* **96**, 212503 (2010).

¹²J. M. Hu and C. W. Nan, *Phys. Rev. B* **80**, 224416 (2009).

¹³H. Béa *et al.*, *Phys. Rev. Lett.* **100**, 017204 (2008); J. Allibe *et al.*, *Appl. Phys. Lett.* **95**, 182503 (2009).

¹⁴S. Geprägs *et al.*, *Appl. Phys. Lett.* **96**, 142509 (2010); M. Weiler *et al.*, *New J. Phys.* **11**, 013021 (2009).

¹⁵J.-W. Lee, S.-C. Shin, and S.-K. Kim, *Appl. Phys. Lett.* **82**, 2458 (2003); S.-K. Kim *et al.*, *J. Magn. Magn. Mater.* **267**, 127 (2003).

¹⁶G. Niu *et al.*, *Appl. Phys. Lett.* **95**, 062902 (2009).

¹⁷D. Esteve *et al.*, *Phys. Status Solidi B* **247**, 1956 (2010).

¹⁸S. Park *et al.* (to be published in *Journal of Physics: Condensed Matter*, 2011).

¹⁹S. Park and D. Ravelosona, 11th Joint MMM Intermag Conference (IEEE Magnetics Society, Washington, DC, USA, 2010).

²⁰D. Ravelosona, *Dynamics of Domain Wall Motion in Wires with Perpendicular Anisotropy*, in *Nanoscale Magnetic Materials and Applications*, edited by P. Liu (Springer Verlag, New York, NY, 2009).

²¹I. Horcas *et al.*, *Rev. Sci. Instrum.* **78**, 013705 (2007).

²²J.-M. Beaujour *et al.*, *J. Appl. Phys.* **109**, 033917 (2011).

²³J. Ferré, *Dynamics of Magnetization Reversal: From Continuous to Patterned Ferromagnetic Films* (Springer-Verlag, Berlin, 2002).

²⁴L. Cagnon *et al.*, *Phys. Rev. B* **63**, 104419 (2001).

²⁵A. A. Levin *et al.*, *J. Appl. Phys.* **103**, 054102 (2008).

²⁶N. Sato, *J. Appl. Phys.* **64**, 6424 (1988); S. Hashimoto, Y. Ochiai, and K. Aso, *ibid.* **66**, 4909 (1989).

²⁷R. C. O'Handley, *Modern Magnetic Materials: Principles and Applications* (Wiley, New York, 2000).

²⁸D. X. Wang *et al.*, *J. Appl. Phys.* **97**, 10C906 (2005).

²⁹K. Wasa *et al.*, *Appl. Phys. Lett.* **88**, 122903 (2006).

³⁰R. K. Zheng *et al.*, *J. Appl. Phys.* **108**, 033912 (2010).